

## FAR-ULTRAVIOLET EMISSION FROM ELLIPTICAL GALAXIES AT $z = 0.33$ <sup>1</sup>

THOMAS M. BROWN, HENRY C. FERGUSON, ED SMITH

Space Telescope Science Institute, 3700 San Martin Drive, Baltimore, MD 21218. tbrown@stsci.edu, ferguson@stsci.edu, edsmith@stsci.edu

CHARLES W. BOWERS, RANDY A. KIMBLE

Code 681, NASA Goddard Space Flight Center, Greenbelt, MD 20771. charles.w.bowers@nasa.gov, randy.a.kimble@nasa.gov

ALVIO RENZINI

European Southern Observatory, Karl-Schwarzschild-Strasse 2, Garching bei München, Germany arenzini@eso.org

R. MICHAEL RICH

Division of Astronomy, Dpt. of Physics & Astronomy, UCLA, Los Angeles, CA 90095. rmr@astro.ucla.edu

*To appear in The Astrophysical Journal Letters*

### ABSTRACT

We present far-ultraviolet (far-UV) images of the rich galaxy cluster ZwCl1358.1+6245, taken with the Space Telescope Imaging Spectrograph on board the Hubble Space Telescope (HST). When combined with archival HST observations, our data provide a measurement of the UV-to-optical flux ratio in 8 early-type galaxies at  $z = 0.33$ . Because the UV flux originates in a population of evolved, hot, horizontal branch (HB) stars, this ratio is potentially one of the most sensitive tracers of age in old populations – it is expected to fade rapidly with lookback time. We find that the UV emission in these galaxies, at a lookback time of 3.9 Gyr, is significantly weaker than it is in the current epoch, yet similar to that in galaxies at a lookback time of 5.6 Gyr. Taken at face value, these measurements imply different formation epochs for the massive ellipticals in these clusters, but an alternative explanation is a “floor” in the UV emission due to a dispersion in the parameters that govern HB morphology.

*Subject headings:* galaxies: evolution – galaxies: stellar content – ultraviolet: galaxies – galaxies: cooling flows

### 1. INTRODUCTION

Elliptical and S0 galaxies show a striking rise in their spectra at  $\lambda < 2000$  Å. Spectroscopy (Brown et al. 1997) and imaging (Brown et al. 2000b) of local galaxies show this “UV upturn” arises from a minority population of hot horizontal branch (HB) stars. On energetic grounds, these evolved stars were long considered the best candidates for the UV emission (Greggio & Renzini 1990), with the implication that the UV-to-optical color could be the most rapidly evolving feature in the spectra of ellipticals. In theory, the UV upturn can fade by several magnitudes as the lookback time increases by a few gigayears, but the evolution is very model-dependent, and a strong UV upturn could appear at ages as early as  $\sim 6$  Gyr (Tantalo et al. 1996) or as late as  $\gtrsim 15$  Gyr (Yi, Demarque, & Oemler 1998).

This evolution has motivated our ongoing survey to measure the UV upturn in clusters at intermediate redshifts. Previously, we observed the rich clusters Abell 370 at  $z = 0.375$  (Brown et al. 1998) and CL0016+16 at  $z = 0.55$  (Brown et al. 2000a); those observations implied that there was little fading of the UV upturn out to  $z \approx 0.4$  with a significant decline at higher  $z$ . However, further cluster measurements are clearly needed to explore the universality of this evolution.

To that end, we have obtained far-UV images of ZwCl1358.1+6245 with the Space Telescope Imaging Spectrograph (STIS) on board the Hubble Space Telescope (HST). This is a rich, compact cluster of galaxies originally identified by Zwicky & Herwig (1968) and later rediscovered in the x-

ray observations of Luppino et al. (1991). It lies at intermediate redshift ( $z = 0.33$ ; Fisher et al. 1998) with little foreground extinction ( $E_{B-V} = 0.023$  mag; Schlegel, Finkbeiner, & Davis 1998). When combined with archival images from the Wide Field Planetary Camera 2 (WFPC2) on HST, our far-UV images provide a measurement of the UV upturn for 8 elliptical and S0 galaxies in the cluster core. Seven of these galaxies are well-detected ( $> 3\sigma$ ) in the far-UV, and the central galaxy shows strong extended UV emission, likely associated with infalling matter. The weak UV upturn measured in these galaxies is in contrast to the strong UV upturn measured previously at  $z = 0.375$ , yet surprisingly similar to that at  $z = 0.55$ .

### 2. OBSERVATIONS AND DATA REDUCTION

#### 2.1. Far-UV Imaging

We imaged ZwCl1358.1+6245 for 68,291 s while the cluster was in the HST Continuous Viewing Zone. The field was centered at an R.A. of  $13^h59^m50.63^s$  and a Dec. of  $62^\circ31'5.3''$  (J2000) with a position angle of  $50^\circ$ , placing 8 S0 and elliptical galaxies within the STIS  $25'' \times 25''$  field, including the brightest galaxy of the cluster (see Figure 1). Exposures were dithered by 1–2 pix to allow removal of hot pixels. We used the F25QTZ filter (1450–1900 Å) to minimize the background from geocoronal emission in H I  $\lambda 1216$  and O I  $\lambda 1304$ . Note that the sensitivity of the far-UV camera has been slowly decreasing at the rate of  $\sim 1.5\%$  yr $^{-1}$ ; we include this decline in our analysis (at the time of our observations, a flat spectrum of  $1.19 \times 10^{-16}$  erg $^{-1}$  s $^{-1}$  cm $^{-2}$  Å $^{-1}$  produced 1 count s $^{-1}$  in this bandpass).

The STIS far-UV detector has a very low dark rate when cold ( $\sim 6 \times 10^{-6}$  cts sec $^{-1}$  pix $^{-1}$ ), but as observations progress, a dark count “glow” appears, centered in the upper left-hand

<sup>1</sup>Based on observations made with the NASA/ESA Hubble Space Telescope, obtained at the Space Telescope Science Institute, which is operated by AURA, Inc., under NASA contract NAS 5-26555. These observations are associated with proposal 8564.

quadrant of the detector. Using the optical images to mask objects, we normalized and subtracted from each exposure a profile of this dark glow (created from a sum of  $\sim 500$  ks of dark exposures). We co-added the exposures using the IRAF DRIZZLE package, weighting the pixels in each frame by the ratio of the exposure time squared to the dark count variance, including a hot pixel mask. The algorithm weights the exposures by the square of the signal-to-noise ratio for sources fainter than the background. Note that the STIS UV detectors are photon counters that register less than 1 count per cosmic-ray hit, and thus the images do not require the cosmic-ray rejection required for processing CCD images.

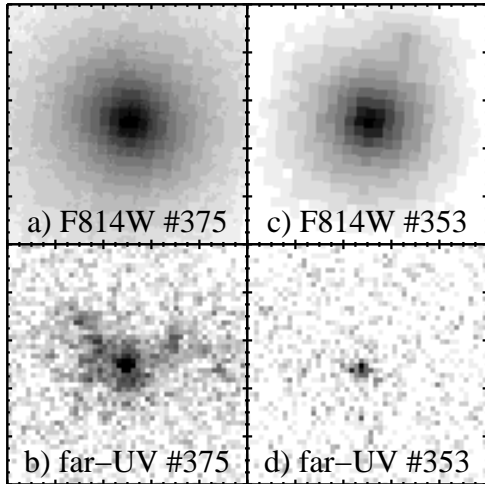


FIG. 1—Optical and far-UV images of two early-type galaxies in ZwCl1358.1+6245 ( $2.5'' \times 2.5''$ ). Ellipticals at low  $z$  usually appear compact in the UV, but the brightest cluster member (panels *a* & *b*) shows irregular structure that is not seen in the optical, likely from Lyman- $\alpha$ . The other galaxies in our sample appear compact in the UV, as in panel *d*.

## 2.2. Optical Data

We used the DRIZZLE package to co-add the archival WFPC2 images of this cluster, reject cosmic rays and hot pixels, and register the co-added optical data to the far-UV image. WFPC2 data in the F606W (broad  $V$ ) and F814W ( $I$ ) bandpasses were available for our entire field; these data come from an impressive mosaic of the cluster by van Dokkum et al. (1998), who also provide morphological classifications for the galaxies in our sample (Table 1). Partial coverage of our field was also available in F450W ( $B$ ). The UV upturn strength is usually measured by the rest-frame  $m_{1550} - V$  color, where the flux from 1250–1850 Å gives  $m_{1550}$  and  $V$  is Johnson  $V$ . Our far-UV bandpass corresponds to rest-frame 1090–1429 Å while the F814W bandpass corresponds roughly to Johnson  $V$  in the rest-frame. In §2.5, we will use the spectral energy distributions of local elliptical galaxies, redshifted to  $z = 0.33$ , to interpret the observed count rates in these bandpasses as  $m_{1550} - V$  colors.

## 2.3. Extended Emission

Due to their low luminosity and sharp profile in the far-UV, elliptical galaxies usually appear point-like in images of distant clusters. What is striking about Figure 1 is the appearance of the brightest cluster member, which shows extended tenuous emission that is not seen in the broad WFPC2 bandpasses at longer wavelengths. The cluster shows significant x-ray luminosity (Stocke et al. 1991), and associated H- $\alpha$  emission (Donahue, Stocke, & Giola 1992). The H- $\alpha$  contours extend outward from the nucleus in three prongs, and two of these trace the far-UV emission when the Donahue et al. (1992) image is aligned to our own, strongly suggesting that the far-UV emission is due to Lyman- $\alpha$  redshifted into the STIS far-UV bandpass. The x-ray and H- $\alpha$  emission were historically taken as evidence of a “cooling flow,” although the presence of cooling gas is now controversial, and this term may be a misnomer. Lyman- $\alpha$  emission is expected to trace the H- $\alpha$  emission in galaxy clusters, whether or not the infalling material is cooling in the historical sense, but it is rarely seen because this emission is lost in the geocoronal Lyman- $\alpha$  emission when observing local clusters. Unfortunately, both the Lyman- $\alpha$  emission and the stellar light peak toward the center of this galaxy, so it is difficult to separately quantify the two.

Another, less likely, source would be star-formation from the infalling material. Normalizing a model spectrum of constant star-formation to the far-UV emission, we find that such star formation would be difficult to detect in the optical images. In any case, the optical images show no evidence of the morphology seen in the far-UV.

TABLE 1: Photometry

ID <sup>a,b</sup>	Morph. <sup>a</sup>	far-UV (cts)	F814W (DN)	$m_{1550} - V$ (mag)
381	E	$147 \pm 27$	$33868 \pm 71$	$4.6 \pm 0.2$
375	E	$2873 \pm 66$	$52928 \pm 89$	$1.9^c \pm 0.1$
368	S0	$163 \pm 49$	$13965 \pm 50$	$3.5^{+0.4}_{-0.3}$
357	E	$-23 \pm 52$	$22068 \pm 57$	$> 5.9$
360	E	$139 \pm 47$	$20255 \pm 55$	$4.1 \pm 0.4$
358	S0	$149 \pm 41$	$17587 \pm 51$	$3.8^{+0.4}_{-0.2}$
354	E	$118 \pm 33$	$17165 \pm 51$	$4.1 \pm 0.3$
353	E	$405 \pm 29$	$48531 \pm 92$	$3.9 \pm 0.1$

<sup>a</sup> Fisher et al. (1998).

<sup>b</sup> van Dokkum et al. (1998).

<sup>c</sup> Contaminated by Lyman- $\alpha$  emission.

## 2.4. Photometry

We performed aperture photometry on the far-UV image using our own IDL software, with a source aperture of radius 16 pixels ( $0.4''$ ) and a sky annulus of radii 80 and 100 pixels, as done previously by Brown et al. (2000a). Each aperture was centered on the bright core of the galaxy, determined from the F814W WFPC2 data. Statistical errors for the photometry include the Poisson contribution from the source counts, the statistical uncertainties in the spatially-varying background, and the effects of the weighted co-addition of the frames (see the previous section). Using the DAOPHOT package in IRAF, we measured the flux in the F814W data (registered via DRIZZLE to the far-UV frame) using the same source and sky apertures. The optical and far-UV photometry are shown in Table 1.

Note that the aperture size does not contribute significant systematic errors in our analysis, whether we are considering measurements at different  $z$  or in different bandpasses. Except for galaxy 375 (which has extended emission), there is little variation in our  $m_{1550} - V$  colors as we reduce the aperture size—they remain uniformly red, with small variations consistent with the statistical uncertainties in Table 1. Measurements of  $m_{1550} - V$  in local ellipticals (Burstein et al. 1988) were performed with a  $10'' \times 20''$  aperture, while our  $0.8''$  diameter aperture would subtend  $\sim 50''$  at the distance of Virgo (characteristic of the

Burstein et al. sample). However, in local galaxies, there is almost no variation in the surface  $m_{1550} - V$  color out to a radius of  $\sim 20''$  (Ohl et al. 1998), and the colors within any aperture are dominated by the core (given the sharply peaked profiles). We also note that in the HST bandpasses, our aperture gives encircled energy agreement at the 5% level for point sources and better agreement for extended sources (Robinson 1997<sup>2</sup>; Holtzman et al. 1995).

### 2.5. UV-to-Optical Colors

The UV upturn is traditionally characterized by the rest-frame  $m_{1550} - V$  color (see Burstein et al. 1988). We used the spectra of three local elliptical galaxies (NGC1399, M60, and M49) to convert the observed STIS and WFPC2 countrates to rest-frame  $m_{1550} - V$ , as done previously in Brown et al. (1998) and Brown et al. (2000a). Our spectra of NGC1399, M60, and M49 have respective  $m_{1550} - V$  colors of 2.05, 2.24, and 3.42 mag (Burstein et al. 1988); despite the substantial range in UV upturn strength, the spectral shape within the far-UV range or within the optical range varies little from galaxy to galaxy. We redshifted these local templates to  $z = 0.33$  and then applied a foreground reddening of  $E(B - V) = 0.023$  mag (Schlegel et al. 1998). We then used the IRAF CALCPHOT routine to calculate the relative countrates for these templates in the STIS/far-UV and WFPC2/F814W bandpasses. The ratios of far-UV to F814W countrates observed in the ZwCl1358.1+6245 galaxies ( $R_{obs}$ ) were then compared to the ratios from the templates ( $R_{template}$ ), and the template with the closest ratio was used to determine the rest-frame  $m_{1550} - V$  (Table 1), using the relation

$$(m_{1550} - V)_{obs} = (m_{1550} - V)_{template} - 2.5 \log(R_{obs}/R_{template}).$$

Except for galaxy 375, all of the galaxies show weak UV upturn emission. Galaxy 375 is contaminated by the Lyman- $\alpha$  emission discussed previously, so the UV upturn emission is really an upper limit on the emission from the evolved HB population. Note that in a much smaller aperture (radius 5 pixels) that excludes much of the Lyman- $\alpha$  emission, this galaxy has an even bluer  $m_{1550} - V$  of 1.6 mag.

We show in Figure 2 the  $m_{1550} - V$  colors measured in galaxy clusters to date. Nearby quiescent ellipticals have been measured by Burstein et al. (1988) in Virgo, Coma, and Fornax. The galaxies at  $z = 0.33$  are from the present work (excluding galaxy 375). Measurements at  $z = 0.375$  are from Faint Object Camera (FOC) observations of Abell 370 (Brown et al. 1998). Measurements at  $z = 0.55$  are from STIS observations of CL0016+16 (Brown et al. 2000a). At each redshift, the observed fluxes have been transformed to rest-frame  $m_{1550} - V$  using the spectra of local elliptical galaxies.

Before proceeding, it is worth noting that the  $z = 0.375$  data may have significant systematic errors – the calibration on the FOC was far less certain than it is with STIS. The measurements at  $z \approx 0$ ,  $z = 0.33$ , and  $z = 0.55$  were all done with distinct photometry in the far-UV and optical, whereas the FOC measurements come from the ratio of two long-pass filters (see Brown et al. 1998). It would be prudent to verify the  $m_{1550} - V$  colors at  $z = 0.375$  with a true solar-blind instrument, such as STIS or the far-UV channel on the Advanced Camera for Surveys, to verify that the UV upturn is so strong in Abell 370.

<sup>2</sup>R. Robinson 1997, Examining the STIS Point-Spread Function, [http://hires.gsfc.nasa.gov/stis/postcal/quick\\_reports.html](http://hires.gsfc.nasa.gov/stis/postcal/quick_reports.html)

### 3. DISCUSSION

To place our observations in context, we have plotted in Figure 2 the models of Tantalo et al. (1996), which were constructed assuming gas infall for the chemical evolution, and under the assumption that massive ellipticals form by monolithic collapse. The onset of the UV upturn is very sensitive to the formation redshift ( $z_f$ ) assumed, and for the moment, we will consider this at face value.

Leaving aside the uncertain result at  $z = 0.375$ , Figure 2 demonstrates that the UV upturn does indeed fade with increasing  $z$ , but does so much more slowly than, for example, in the models of Tantalo et al. (1996). In fact, very little  $m_{1550} - V$  evolution appears to exist between  $z = 0.33$  and 0.55. Given the  $m_{1550} - V$  range observed at  $z = 0$ , correlated with metallicity, the trend is most apparent if one considers both the mean and the most blue  $m_{1550} - V$  in each epoch; there are enough galaxies to imply that the UV upturn is systematically weaker at  $z = 0.33$  and 0.55. The figure suggests that galaxies in the  $z = 0.33$  cluster formed at  $z \sim 2$ , while those in the  $z = 0.375$  and 0.55 clusters formed at  $z \sim 4$ . Given the evidence for hierarchical merging, such variation may not be inconceivable. However, we have targeted the massive ellipticals in the centers of rich clusters, with no spectroscopic evidence of recent star formation. The UV upturn traces the age of the oldest stars in these populations, not necessarily the ages of the galaxies. If these galaxies formed via monolithic collapse, the age of the oldest stars reflects the age of the galaxies themselves, but if the galaxies formed via hierarchical merging, the oldest stars may predate the merger events and still comprise the bulk of the population. Studies of clusters out to  $z \sim 1$  indicate that most of the star formation in ellipticals had to be completed at  $z \gtrsim 3$ , followed by quiescent evolution (Stanford, Eisenhardt, & Dickinson 1998; Kodama et al. 1998). Therefore, we expect little scatter in  $z_f$ . In contrast, the strong distinction between the measurements at  $z = 0.33$  and 0.375, and, more importantly, the similarity between the measurements at  $z = 0.33$  and 0.55, implies a surprisingly large dispersion in the formation epochs between clusters ( $z_f \approx 2 - 4$ ). Such variation in  $z_f$  would be more plausible if the nonmonotonic evolution in  $m_{1550} - V$  implied by the FOC measurements were independently confirmed.

Another (less likely) explanation for the variation in Figure 2 is that there is a small dispersion in  $z_f$  among the clusters, but the chemical evolution varied significantly from cluster to cluster. The onset of the UV upturn in the Tantalo et al. (1996) models depends upon the details of the chemical evolution, and the UV upturn in local ellipticals correlates strongly with metallicity, and to a lesser extent, with luminosity (Burstein et al. 1988). However, all of the galaxies in these programs are massive ellipticals in the centers of rich, massive clusters – it seems unlikely that their populations would be chemically distinct from their analogs in the local Universe. Even so, it would be interesting to obtain metallicity measurements for our sample, to look for trends like those seen locally.

Models for the evolution of elliptical galaxies are sensitive not only to  $z_f$ , but to other parameters, such as time of onset for galactic winds, accretion timescale, and efficiency of star formation. Tantalo et al. (1996) tuned these parameters to reproduce the properties of low- $z$  ellipticals, and there is not much freedom to tune them further to match our observed UV evolution. It is therefore worth looking at the parameters that affect HB morphology in particular. Hot HB stars have lost nearly all (but not all) of their envelope due to mass loss on the RGB.

Tantalo et al. (1996) make specific assumptions about the relation between mass loss and chemical abundance in order to approximate the UV upturn range at  $z = 0$ . In their models, hot HB stars do not exist at higher  $z$  because their main sequence progenitors have larger masses (resulting in redder HB stars). What if, instead, we imagine that at  $z = 0$  there is a reservoir of stars in ellipticals that have lost so much mass that they fail to ignite He? See, e.g., Figure 9 in Greggio & Renzini (1990). These stars could, for example, come from the high-metallicity tail of the metallicity distribution. At higher  $z$ , the more massive stars in that metallicity range would become hot HB stars, providing the UV flux that would otherwise be missing. Therefore, moving from zero to high redshift, the UV upturn would be produced by stars at progressively higher metallicity, until it disappears entirely when the very end of the metallicity distribution is reached. In more general terms, the same qualitative behavior is expected if the occurrence of hot HB stars is driven by a distribution of stellar ages, or a distribution of RGB mass loss, or a combination thereof. It is plausible that the details of the metallicity distribution, and the relation between mass loss and RGB parameters, could be tuned to reproduce the gradual  $m_{1550} - V$  evolution observed, with a common  $z_f \sim 4$ , without violating other constraints on stellar evolution.

Further alternatives are also possible. At  $z = 0$ , hot HB stars may be the dominant, but not the sole, contributor to the UV upturn. While the hot HB would rapidly disappear with redshift, the  $m_{1550} - V$  color would initially drop, but then hit a *floor* value as the role of dominant UV contributor is assumed by another class of UV-bright objects whose evolution with redshift is not as fast as that of the hot HB stars. Possibilities include a low level of ongoing (massive) star formation, and various kinds of binaries such as, e.g., post-RGB binary components and accreting white dwarfs (Greggio & Renzini 1990). If future observations can show that HB stars are not the sole contributor to the UV upturn at  $0.3 \lesssim z \lesssim 0.6$ , the Tantalo et al. (1996) models would imply  $z_f \lesssim 2$ ; however, given that Kodama et al. (1998) and Stanford et al. (1998) find the bulk of the stellar population formed at  $z_f \gtrsim 3$ , such a finding would more likely tell us that the onset of the UV upturn takes place at an older age than the  $\sim 6$  Gyr given by the models of Tantalo et al. (1996).

It would be difficult to rule out a low star formation rate (SFR) as the source of the  $m_{1550} - V$  floor. Assuming constant star formation with a flat  $f_\nu$  spectrum, the Kennicutt (1998) relation gives  $\text{SFR} = 1.4 \times 10^{-28} L_\nu \approx 0.005 - 0.02 M_\odot \text{ yr}^{-1}$  for our  $z = 0.33$  sample (excluding galaxies 375 and 357). This is a lower limit, given that the real spectrum would likely have a far-UV downturn due to extinction. The rates in the galaxies at  $z = 0.55$  are similar ( $0.008 - 0.015 M_\odot \text{ yr}^{-1}$ ). Thus, from  $z = 0.6$  to  $z = 0.3$  (a span of 2.4 Gyr), this SFR would pro-

duce  $\sim 3 \times 10^7 M_\odot$  of stars, which would be at least 3.6 Gyr old today if the star formation stopped at  $z = 0.3$ . A remnant intermediate-age population comprising a few percent of the total stellar mass in a normal elliptical galaxy would be difficult to detect. The same arguments apply if the star formation is episodic, because the number of  $> 3\sigma$  detections at  $z = 0.33$  (excluding galaxy 375) and  $z = 0.55$  implies a duty cycle of  $\sim 80\%$ . This hypothesis could be tested by searching for low levels of H- $\alpha$  or O II emission.

In summary, our findings are in broad agreement with the expectation of a fading UV upturn with redshift, due to a progressively smaller number of hot HB stars being produced in younger populations. However, the rate of this fading remains to be understood – whether the whole trend can be attributed to the redshift evolution of the number of hot HB stars, or whether an additional class of hot stars is contributing a floor to the UV flux that is minor at  $z = 0$  but already dominant at  $z \sim 0.3$ .

Support for proposal 8564 was provided by NASA through a grant from the Space Telescope Science Institute, which is operated by AURA, Inc., under NASA contract NAS 5-26555. We are grateful to A.V. Sweigart for useful discussions.

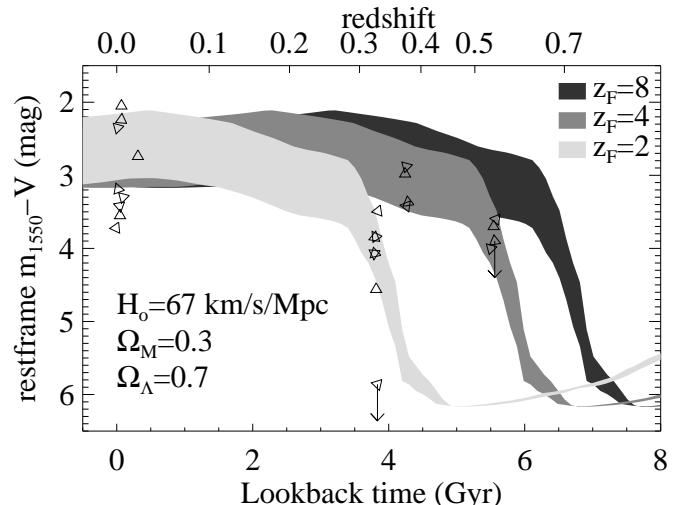


FIG. 2—Evolution of the rest-frame  $m_{1550} - V$  color according to the models of Tantalo et al. (1996) (shaded), assuming a reasonable cosmology and three different epochs of galaxy formation (labeled). The sudden onset of UV emission is caused by the appearance of metal-rich hot HB stars, with the spread in colors bounded by models at  $M = 3 \times 10^{12}$  and  $M = 10^{12} M_\odot$ . The timing of the onset is much more sensitive to  $z_f$  than to the cosmological parameters. The triangles represent the colors measured to date for quiescent E and S0 galaxies. The statistical uncertainties (Table 1) are small with respect to the variation from cluster to cluster, except for the  $1\sigma$  limits shown (arrows).

## REFERENCES

Brown, T.M., Bowers, C.W., Kimble, R.A., & Ferguson, H.C. 2000a, ApJ, 529, L89  
 Brown, T.M., Bowers, C.W., Kimble, R.A., Sweigart, A.V., & Ferguson, H.C. 2000b, ApJ, 532, 308  
 Brown, T.M., Ferguson, H.C., Davidsen, A.F., & Dorman, B. 1997, ApJ, 482, 685  
 Brown, T.M., Ferguson, H.C., Deharveng, J.-M., & Jedrzejewski, R.I. 1998, ApJ, 508, L139  
 Burstein, D., Bertola, F., Buson, L.M., Faber, S.M., & Lauer, T.R. 1988, ApJ, 328, 440  
 Donahue, M., Stocke, J.T., Giola, I.M. 1992, ApJ, 385, 49  
 Fisher, D., Fabricant, D., Franx, M., & van Dokkum, P. 1998, ApJ, 195, 212  
 Greggio, L., & Renzini, A. 1990, ApJ, 364, 35  
 Holtzman, J., et al. 1995, PASP, 107, 156  
 Kennicutt, R.C., Jr. 1998, ARAA, 36, 189  
 Kodama, T., Arimoto, N., Barger, A.J., & Aragon-Salamanca, A. 1998, A&A, 334, 99  
 Luppino, G.A., Cooke, B.A., McHardy, I.M., & Ricker, G.R. 1991, AJ, 102, 1  
 Ohl, R.G., et al. 1998, ApJ, 505, L11  
 Schlegel, D.J., Finkbeiner, D.P., & Davis, M. 1998, ApJ, 500, 525  
 Stanford, S.A., Eisenhardt, P.R., & Dickinson, M. 1998, ApJ, 492, 461  
 Stocke, J.T., Morris, S.L., Giola, I.M., Maccacaro, T., Schild, R., Wolter, A., Fleming, T.A., & Patrick, H.J. 1991, ApJS, 76, 813  
 Tantalo, R., Chiosi, C., Bressan, A., & Fagotto, F. 1996, A&A, 311, 361  
 van Dokkum, P.G., Frankx, M., Kelson, D.D., Illingworth, G.D., Fisher, D., & Fabricant, D. 1998, ApJ, 500, 714  
 Yi, S., Demarque, P., & Oemler, A. Jr. 1998, ApJ, 492, 480  
 Zwicky, F., & Herzog, E. 1968, Catalogue of Galaxies and of Clusters of Galaxies, Vol. IV (Pasadena: California Institute of Technology), 125